6 December 1996

ELSEVIER

Chemical Physics Letters 263 (1996) 63-72

CHEMICAL PHYSICS LETTERS

Ab initio calculations of the ground and excited states of I_2^- and ICl^-

P.E. Maslen [1], J. Faeder, R. Parson

JILA and Department of Chemistry and Biochemistry, University of Colorado and National Institute of Standards and Technology, Boulder, CO 80309-0440, USA

Received 16 July 1996; in final form 26 September 1996

Abstract

We performed all-electron ab initio calculations of the first six states of I_2^- and ICl^- using a multi-reference configuration interaction method. Spin–orbit coupling is included via an empirical one-electron operator and has a large effect on the dissociation energy. The ground state dissociation energies were in error by 20–30%, probably due to deficiencies in the one electron basis sets. The electronic wavefunctions at the equilibrium geometry were used to calculate the electronic absorption spectrum from the ground state, and good agreement was found with the experimental data.

1. Introduction

Many experiments have probed the dynamics of dissociation and recombination in halogen molecule ions [1–3]. While a primary focus of these experiments is on the effects of solvation, a firm knowledge of the electronic structure of the bare anions is often required to interpret the results. In addition to the energetics of the states involved, it is also necessary to know something about the wavefunction, and hence properties, of the molecules as they dissociate and recombine, in order to determine how the solvent interacts with these states.

There is relatively little experimental information about the ground and excited states of I_2^- and ICl^-. The bond dissociation energy of the ground state is known reasonably well for both molecules from recent photodissociation measurements [4], although there is considerable variation in the reported values estimated from earlier charge-transfer data [5–8]. Absorption spectra with absolute cross sections from photodissociation experiments have also been reported for the band around 700 nm [1,4]. The only other gas phase data available are from dissociative electron attachment measurements [9,10], which yield information about the anion curves near the neutral geometry.

For I_2^- the electronic absorption spectrum and the frequencies of several vibrational transitions have been measured both in crystal matrices and solution [11,12]. Chen and Wentworth [5] have combined the experimental data for most of the diatomic halogen anions to create semiempirical potential energy curves for all of the states considered here. Recently, Dojahn et al. [13] have improved these fits by incorporating newer data. It is important to point out, however, that while these fits combine the available experimental data, there are no direct experimental measurements of most of the spectroscopic quantities that are extracted from these curves. Only the transi-

[1] Current address: Department of Chemistry, University of California, Berkeley, CA 94720, USA.

PII S0009-2614(96)01162-1

tion energies, the vertical electron affinities, the bond dissociation energy of the ground electronic state, and vibrational frequencies of the ground electronic state have been measured directly. For example, the equilibrium bond length of the ground electronic state was estimated by summing the ionic and covalent radii of iodine [13]. It is also unknown what effect matrices or solutions have on the measurements to which the curves were fit.

Less data is available for ICl^-. The only electronic absorption spectrum other than the single band cited above was measured in solution by Shida et al. [12] The observed peak positions are nearly identical to those reported for I_2^- in the same work, a result which is inconsistent with the limited gas phase data [4] and the present calculations.

There have also been few ab initio calculations performed on either of these molecules, and none, to our knowledge, include the effects of spin–orbit coupling. The first calculations on both molecules were due to Tasker et al. [14] with a valence bond method using core potentials and a small basis consisting of only s and p functions. This is the only calculation of ICl^- of which we are aware. The excited states were calculated and transition energies were reported, but without the inclusion of spin–orbit coupling it is difficult to assess the meaning of these energies. For example, the $^2\Pi_{3/2}$ and $^2\Pi_{1/2}$ states of these molecules, which are degenerate in the absence of spin–orbit coupling, are split by about 0.5 eV. Bowmaker et al. performed calculations of I_2^- at the SCF level [15]. More recently, Danovich et al. used relativistic core potentials to study the effects of different methods and basis sets in calculations on I_2^- and several other iodo-containing species [16]. They reported results for the ground state, comparable to our results but omitting spin–orbit coupling. While their dissociation energies show fortuitous agreement with experiment, our experience is that inclusion of spin–orbit coupling reduces the calculated dissociation energies by as much as 50%.

We have performed multireference configuration interaction (MRCI) calculations of the ground and excited states of these ions and incorporated the effects of spin–orbit coupling by adding an empirical one-electron operator to the ab initio Hamiltonian. The results represent the most complete theoretical treatment of these ions to date, and, when combined with the experimental information currently available, should provide improved semiempirical models. The outline of this Letter is as follows. Section 2 describes the methods used to obtain the electronic structure of the ions. The method used for computing the electronic absorption spectra is also described. Section 3 presents the results of the calculations with comparisons to experiments and previous calculations.

2. Methods

The ab initio calculations were performed with the MOLPRO program [17], using the internally contracted multi-reference CISD method developed by Knowles and Werner [18,19]. The orbitals and reference configurations were obtained from state-averaged complete active space (CASSCF) calculations [20,21] including the lowest two Σ states, the lowest two Π_x states, and the lowest two Π_y states. The six states arise from the ^2P states of the neutral halogen and the ^1S state of the halogen ion. All six states were assigned equal weight during the orbital optimization.

Effective core potentials were avoided in favor of all-electron basis sets, largely because of doubts about the accuracy of the available core potentials for iodine. The medium-sized polarized basis sets of Sadlej [22,23] were used in all of the calculations. The suggested additional polarization functions have also been included so that the basis sets are (13s10p4d)/[7s5p2d] and (19s15p12d4f)/[11s9p6d2f] for Cl and I respectively. In order to roughly equalize the error in the CISD electron affinities of Cl and I, the orbital exponents of chlorine's first contracted d function (0.9528 and 0.3580) have been scaled by 0.9195. The resulting exponents are 0.8761 and 0.3292.

To reduce the cost of the CASSCF calculations, the inner orbitals of the dihalides were optimized via a single-reference all-electron SCF calculation, and then frozen during the CASSCF calculation. During the CISD calculation, only the six valence p orbitals were correlated. Including the valence s orbitals in the correlation space had only a small effect, decreasing the well depth for the ground state of I_2^- by 18 meV, or 2%. We opted to exclude the valence s orbitals from the correlation space because basis set superposition error rises very rapidly with the number of correlated

Table 1
Number of active orbitals belonging to each irrep. of the C_{2v} point group for ICl^- and I_2^-

Molecule	Method	A_1	B_1	B_2	A_2
ICl^-	SCF	18	8	8	2
	CASSCF	8	4	4	1
	CISD	2	2	2	0
I_2^-	SCF	26	12	12	4
	CASSCF	18	8	8	2
	CISD	2	2	2	0

electrons, and is especially problematic for weakly bound homonuclear molecules.

Table 1 contains the number of active orbitals in the SCF, CASSCF and CISD calculations. Size consistency errors inherent in the CISD energy were ameliorated by adding an approximate cluster correction due to Pople. The charge distributions of the wavefunctions were obtained using the distributed multipole analysis (DMA) developed by Stone [24].

The ab initio calculations leave out spin–orbit coupling. To include spin–orbit effects, we set up and diagonalize an effective Hamiltonian matrix

$$\mathbf{H}_{\text{eff}} = \mathbf{H}_{\text{a}} + \mathbf{H}_{\text{eff}}^{\text{SO}}, \tag{1}$$

where $\mathbf{H}_{\text{a}}$ is the ab initio Hamiltonian and $\mathbf{H}_{\text{eff}}^{\text{SO}}$ is a semiempirical Hamiltonian described below. Since spin must be considered, the basis for this Hamiltonian consists of a direct product of the six spatial wavefunctions obtained from the ab initio calculation with the doublet spin functions α and β, resulting in 12 basis states. $\mathbf{H}_{\text{a}}$ is thus a diagonal 12×12 matrix with the ab initio energies in degenerate pairs on the diagonal.

The spin–orbit coupling between these basis states is approximated by the one electron Hamiltonian [25]

$$\mathbf{H}_{\text{eff}}^{\text{SO}} = \sum_i \frac{\alpha^2}{2} \left(\frac{Z_A}{r_{iA}^3} \boldsymbol{l}_{iA} + \frac{Z_B}{r_{iB}^3} \boldsymbol{l}_{iB} \right) \cdot \boldsymbol{s}_i, \tag{2}$$

where $\boldsymbol{l}_{iN}$ is the orbital angular momentum of electron i about nucleus N, etc. In principle, the matrix elements of this operator could be evaluated exactly from the ab initio wavefunctions and the spin components. Such a procedure would, however, be very unlikely to give the correct asymptotic spin–orbit splittings for the atoms. We chose instead to approximate the Z/r^3 operators with the experimental values for the appropriate atomic spin–orbit coupling constants, ζ, so that

$$\mathbf{H}_{\text{eff}}^{\text{SO}} \approx \sum_i \frac{\alpha^2}{2} (\zeta_A \boldsymbol{l}_{iA} + \zeta_B \boldsymbol{l}_{iB}) \cdot \boldsymbol{s}_i.$$

Evaluating this operator involves matrix elements of the spin angular momentum operator, which are just the components of the 2×2 Pauli spin matrices, together with matrix elements of the orbital angular momentum operator, which were evaluated exactly using the ab initio wavefunctions. Because the radial operator Z/r^3 decays rapidly as the electron moves away from the nucleus, matrix elements of the spatial part of the spin-orbit operator connecting atomic orbitals on different nuclei were set to zero. In practice two-center integrals were excluded by setting to zero the two-center contributions to the ab initio one particle density matrices.

This procedure gives the exact asymptotic values for the atomic spin–orbit splittings, because the angular integrals attain their correct values at large internuclear separations through symmetry. As the atoms are brought together the spin–orbit coupling varies *only* because (1) the energy separations between the basis states change, and (2) the atomic angular momenta $\boldsymbol{l}_A$ and $\boldsymbol{l}_B$ change. The radial components ζ_A and ζ_B are held fixed at the atomic values.

Electronic absorption spectra from the ground electronic and vibrational states are computed from the calculated curves and transition moments using a slightly modified form of the reflection approximation[26] described by Heller [27]. The total absorption cross section at frequency ω from the initial state i to the final state f is given by

$$\sigma_{\text{if}}(\omega) = 4\pi^2 \alpha a_0^2 \omega \left| V_{\text{f}}'(q_{\text{T}}) \right|^{-1} |\mu_{\text{if}}(q_{\text{T}}) \psi_{\text{i}}(q_{\text{T}})|^2, \tag{3}$$

where V_{f} is the upper state potential, q_{T} is the classical turning point on the upper state, and μ_{if} and ψ_{i} are the transition moments and ground state vibrational wavefunctions respectively. For a given ω and initial state energy E_{i}, the classical turning point is defined by $\hbar\omega = V_{\text{f}}(q_{\text{T}}) - E_{\text{i}}$. We have approximated the ground vibrational state by a harmonic oscillator of frequency ω_{e}, determined from the calculated ground state curve, a minor approximation given the small anharmonici-

ties of the ground states (see Section 3). This method is convenient, and, though approximate, should give good results for our application. As a test, we have computed the absorption spectrum of ICl^- using an exact time-dependent quantum method and found deviations much smaller than the expected accuracy of the electronic structure calculations.

3. Results and discussion

The calculated ab initio potential curves for the lowest six electronic states of I_2^- and ICl^- are shown in Fig. 1. The curves in part (a) of the figure represent the raw data from the ab initio calculation, which does not include spin–orbit coupling. These Hund's case (a) basis states are used to construct the effective spin–orbit Hamiltonian described in Section 2. All of the states considered here correspond to a hole in a p atomic orbital on either I or Cl. In the bonding region, this correlates to a hole in either a σ^* or π^* anti-bonding orbital, giving rise to the bonding Σ and Π states respectively, or to a hole in σ or π bonding orbitals, giving rise to the Σ^* and Π^* states. In I_2^- the Hund's case (a) basis states are degenerate at infinite separation, corresponding to $I^- + I\ (^2P)$. In ICl^- the asymptotic energies correspond to $Cl^- + I\ (^2P)$ and $I^- + Cl\ (^2P)$, and they are split by the electron affinity difference between I and Cl. The calculated value of this difference, 0.596 eV, compares reasonably well with the experimental value of 0.553 eV [28], though it should be noted that the basis set was adjusted to minimize the discrepancy.

The Hund's case (a) curves illustrate several important points. First, there is a strong attractive interaction in the Σ bonding state, while the remaining curves are repulsive or only slightly attractive. Second, the Σ^* anti-bonding state lies above the Π^* anti-bonding state at the equilibrium bond length, R_e, which will strongly influence the character of the spin–orbit coupled excited states, as discussed below. Finally, there is a crossing between the Σ^* and Π^* states at intermediate bondlengths which is due to the interaction between the positive quadrupole moment of the neutral atom and negative charge of the ion. This interaction is attractive for the Σ states, and repulsive for the Π states.

The inclusion of spin–orbit coupling splits the four Hund's case (a) levels into six, and lifts the degeneracy of the atomic $^2P_{3/2}$ and $^2P_{1/2}$ states, giving rise to two asymptotes in I_2^- and four asymptotes in ICl^-, as illustrated in Fig. 1b. Although the Hund's case (a) labels are still used to describe the curves, only Ω, the projection of the total electronic angular momentum onto the internuclear axis, remains valid. In I_2^- the g and u parity labels also remain valid. The mixing of the Σ and Π states by spin–orbit coupling has an important experimental manifestation in that it provides oscillator strength to electronic transitions that would otherwise be expected to be very weak. The extent of this mixing at different bondlengths is discussed below.

Tables 2 and 3 present the spectroscopic constants extracted from the potential curves and also a comparison with previous experimental and theoretical results. We have not presented the vertical electron affinities of I_2 or ICl, because the ab initio calculations do not converge well for bondlengths much shorter than R_e. As can be seen from Fig. 1, the equilibrium bondlength of the neutral is in both cases considerably shorter than that of the ion.

Comparison of calculated and measured bond dissociation energies in the ground state shows that the calculated D_e is in error by about 20-30%. This shortfall is probably due to inadequacies in the one electron basis sets. Teichteil and Pelissier [29] have reported similar problems in obtaining accurate results for D_e in I_2. There is somewhat less discrepancy in the values of ω_e for I_2^-, but direct comparison is hindered by the fact that the experimental values are from the condensed phase [30]. There is good agreement between the current results without spin–orbit coupling and the best previous calculation [16], but the good agreement between the results neglecting spin–orbit coupling and experiment is fortuitous. Neglecting spin–orbit coupling raises the energy of the asymptote with respect to the well because the mixing is much stronger at long bondlengths where the Hund's case (a) states are degenerate. There is reasonable agreement in the calculated and estimated values of R_e for I_2^- [13], but the actual values of R_e are unknown. Danovich et al. [16] reported a slightly shorter bondlength, which may be due to their use of effective core potentials, or to our neglect of other relativistic effects.

The excited state curves are all unbound or very

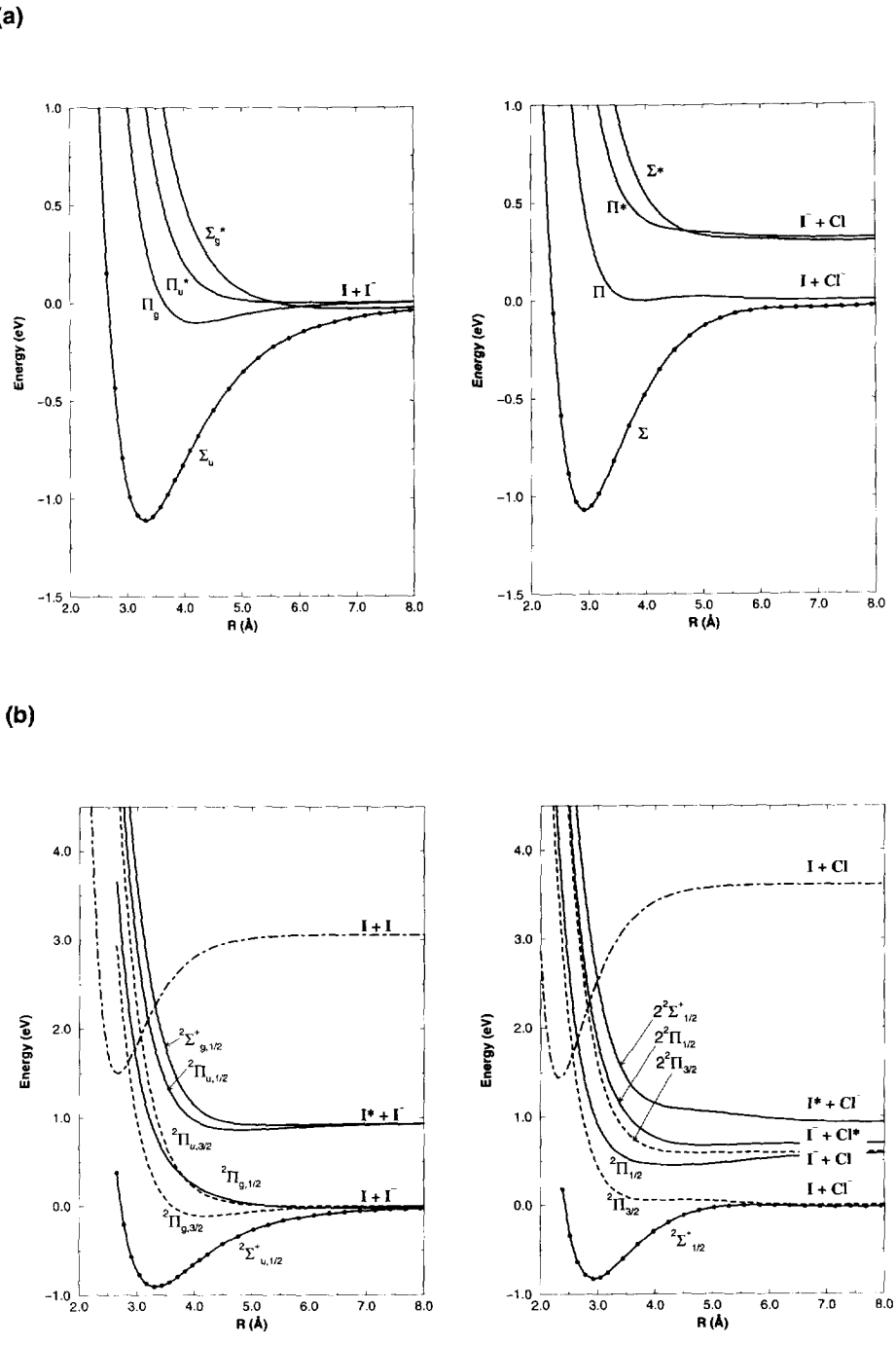

Fig. 1. Ab initio potential curves for ICl^- and I_2^-. (a) Without spin–orbit coupling. (b) Including spin–orbit coupling. The Hund's case (a) labels used in (b) are approximately valid near R_e, but become inappropriate as the bond dissociates (see Tables 5 and 6). Parameters for the neutral curves were taken from Ref. [31].

Table 2
Spectroscopic constants for I_2^-

State		T_e (eV)	R_e (Å)	D_e (eV)	ω_e (cm^{-1})
$^2\Sigma^+_{u,1/2}$	current calc.	0.0	3.33	0.905	99.9[a]
	w/o spin–orbit coupling	0.0	3.35	1.111	105.9
	prev. calc. w/o s.o.c.[b]	0.0	3.23	1.111	112.6
	semi-empirical[c]	0.0	3.39	1.055	115
	exp.	0.0	–	1.18[d]	115[e]
$^2\Pi_{g,3/2}$	current calc.	1.17	4.18	0.11	38
	semi-empirical[c]	1.08	4.10	0.22	44
$^2\Pi_{g,1/2}$	current calc.	1.71	unbound		
	semi-empirical[c]	1.53	4.63	0.08	24
$^2\Pi_{u,3/2}$	current calc.	1.96	unbound		
	semi-empirical[c]	1.55	4.63	0.10	30
$^2\Pi_{u,1/2}$	current calc.	2.66	4.79	0.08	25
	semi-empirical[c]	2.12	4.11	0.19	46
$^2\Sigma^+_{g,1/2}$	current calc.	3.14	5.40	0.025	12
	semi-empirical[c]	3.10	5.41	0.10	22

[a] $\omega_e x_e = 0.35\ cm^{-1}$.
[b] Ref. [16]. QCISD using relativistic effective core potentials.
[c] Ref. [13]. [d] Ref. [4].
[e] Ref. [30]. Measured in solution. $\omega_e x_e = 0.45\ cm^{-1}$.

Table 3
Spectroscopic constants for ICl^-

State		T_e (eV)	R_e (Å)	D_e (eV)	ω_e (cm^{-1})
$^2\Sigma^+_{1/2}$	current calc.	0.0	2.93	0.831	179.5[a]
	w/o spin–orbit coupling	0.0	2.92	1.068	184.1
	prev. calc. w/o s.o.c.[b]	0.0	3.07	0.73	159[c]
	exp.	0.0	–	1.01[d]	–
$^2\Pi_{3/2}$	current calc.	1.39	unbound		
$^2\Pi_{1/2}$	current calc.	1.88	4.34	0.14	33
$2\,^2\Pi_{3/2}$	current calc.	2.67	unbound		
$2\,^2\Pi_{1/2}$	current calc.	2.91	4.88	0.028	31
$2\,^2\Sigma^+_{1/2}$	current calc.	3.62	unbound		

[a] $\omega_e x_e = 0.90\ cm^{-1}$.
[b] Ref. [14]. Valence bond using small basis set and nonrelativistic core potentials.
[c] $\omega_e x_e = 0.9\ cm^{-1}$. [d] Ref. [4].

Table 4
Calculated absorption spectra from the ground electronic state compared with various experimental results

Excited state			Peak position		Peak cross section	FHWM	Integrated intensity
			(eV)	(nm)	(Å^2)	(eV)	(relative units)
I_2^-	$^2\Pi_{g,3/2}$	calc.	1.16	1070	0.0016	0.16	1/280
		matrix [a]	1.08	1150		0.19	1/56
		solution [b]	1.20	1030			
	$^2\Pi_{g,1/2}$	calc.	1.69	736	0.43	0.18	1.0
		matrix [a]	1.55	800		0.22	1.0
		solution [b]	1.68	737			
		direct [c]	1.65	750	0.5	0.18	
	$^2\Sigma^+_{g,1/2}$	calc.	3.12	397	1.3	0.35	5.6
		matrix [a]	3.10	400		0.55	6.1
		solution [b]	3.13	395			
ICl^-	$^2\Pi_{3/2}$	calc.	1.36	914	0.00015	0.24	1/71
		solution [b]	1.20	1030			
	$^2\Pi_{1/2}$	calc.	1.83	676	0.039	0.25	1
		solution [b]	1.68	737			
		direct [d]	1.77	700	0.039	0.23	
	$2\,^2\Pi_{3/2}$	calc.	2.66	467	0.00097	0.46	1/22
	$2\,^2\Pi_{1/2}$	calc.	2.83	438	0.068	0.44	3.0
	$2\,^2\Sigma^+_{1/2}$	calc.	3.59	346	0.63	0.56	36
		solution [b]	3.22	385			

[a] Ref. [11]. [b] Ref. [12]. [c] Ref. [1]. [d] Ref. [4].

weakly bound in comparison with the ground state, as one would expect from simple molecular orbital considerations. Through comparison with the known bond dissociation energies of Xe_2^+, Dojahn et al. [13] have suggested that all of the excited states of I_2^- are slightly bound. Given the limits of the current calculations, we do not expect these wells to be accurately reproduced, and there is considerable discrepancy between our calculated values and the semiempirical fits.

There is considerably better agreement in the values of the electronic transition energies from the ground state (T_e). Direct comparison of the simulated spectra with experimental data is shown in Table 4. For the three optically allowed transitions of I_2^-, the agreement is quite good. Particularly encouraging is the agreement with the positions, widths, and absolute cross sections of the $^2\Pi_{1/2}$ absorption bands observed by gas phase photodissociation [1,4]. Because the $\Sigma \rightarrow \Pi$ transition moment is very small, almost all the oscillator strength of this band is derived from $\Pi \leftrightarrow \Sigma^*$ mixing induced by the spin–orbit coupling. The absolute cross section should thus be quite sensitive to the extent of this mixing, and the good agreement, to within the reported experimental error, suggests that this mixing is about right at R_e. The calculated extent of this mixing is shown at several bondlengths in Tables 5 and 6. The fact that this mixing is much smaller in ICl^- mostly accounts for the order of magnitude reduction in both the calculated and observed cross sections.

There is more significant disagreement in the excitation energies to the two excited states of Π_u symmetry in I_2^-. This transition is dipole forbidden, so its appearance at 585 nm (2.12 eV) in the matrix absorption spectra means that the crystal field must be causing significant mixing with states of g symmetry. It is not known whether this mixing shifts the energy of the Π_u state significantly, or whether the state involved is the $\Pi_{u,3/2}$ or the $\Pi_{u,1/2}$. Chen and Wentworth [5,13] have assigned the 585 nm transition to the $\Pi_{u,1/2}$ state, but if the assignment were changed to $\Pi_{u,3/2}$, the agreement with our calculations would be considerably better. There is evidence from the solution data [12] for an additional absorption band around 480 nm (2.58

Table 5
Case (a) composition of the spin–orbit coupled states of I_2^- as a function of the bondlength

State	R (Å)	% Basis function character			
		Σ_u	Σ_g^*	Π_g	Π_u^*
$^2\Sigma^+_{u,1/2}$	R_e	95.9	0.0	0.0	4.1
	5.3	77.7	0.0	0.0	22.3
	∞	66.7	0.0	0.0	33.3
$^2\Pi_{g,3/2}$	R_e	0.0	0.0	100.0	0.0
	5.3	0.0	0.0	100.0	0.0
	∞	0.0	0.0	100.0	0.0
$^2\Pi_{g,1/2}$	R_e	0.0	9.8	90.2	0.0
	5.3	0.0	63.4	36.6	0.0
	∞	0.0	66.7	33.3	0.0
$^2\Pi_{u,3/2}$	R_e	0.0	0.0	0.0	100.0
	5.3	0.0	0.0	0.0	100.0
	∞	0.0	0.0	0.0	100.0
$^2\Pi_{u,1/2}$	R_e	4.1	0.0	0.0	95.9
	5.3	22.3	0.0	0.0	77.7
	∞	33.3	0.0	0.0	66.7
$^2\Sigma^+_{g,1/2}$	R_e	0.0	90.2	9.8	0.0
	5.3	0.0	36.6	63.4	0.0
	∞	0.0	33.3	66.7	0.0

Table 6
Case (a) composition of the spin–orbit coupled states of ICl^- as a function of the bondlength

State	R (Å)	% Basis function character			
		Σ	Σ^*	Π	Π^*
$^2\Sigma^+_{1/2}$	R_e	96.6	0.0	2.8	0.6
	5.3	68.6	3.9	25.7	1.8
	∞	66.7	0.0	33.3	0.0
$^2\Pi_{3/2}$	R_e	0.0	0.0	99.0	1.0
	5.3	0.0	0.0	96.9	3.1
	∞	0.0	0.0	100.0	0.0
$^2\Pi_{1/2}$	R_e	2.4	1.6	94.0	2.1
	5.3	17.0	47.3	24.4	11.4
	∞	0.0	66.7	0.0	33.3
$2\,^2\Pi_{3/2}$	R_e	0.0	0.0	1.0	99.0
	5.3	0.0	0.0	3.1	96.9
	∞	0.0	0.0	0.0	100.0
$2\,^2\Pi_{1/2}$	R_e	1.0	3.6	1.1	94.3
	5.3	0.1	28.6	7.6	63.0
	∞	0.0	33.3	0.0	66.7
$2\,^2\Sigma^+_{1/2}$	R_e	0.1	94.8	2.1	3.0
	5.3	13.7	20.2	42.4	23.8
	∞	33.3	0.0	66.7	0.0

eV), which supports this alteration in the assignment.

There is also some disagreement between the calculated absorption spectrum for ICl^- and the spectrum measured in solution [12]. The solution data show almost no shift in the spectra between I_2^- and ICl^-, which disagrees qualitatively with the current calculations. The origin of this discrepancy is unknown, but the good results for I_2^- combined with the good agreement for the $^2\Pi_{1/2}$ absorption of ICl^- measured by photodissociation provide some weight for the validity of the current calculations.

It is interesting to examine the extent of the mixing induced by spin–orbit coupling. While this coupling has a large effect on the energies of the curves at all bondlengths studied, the basic Hund's case (a) character of the states is retained at R_e, as can been seen from Tables 5 and 6. Mixing increases rapidly as the bond is stretched. In all the states which are substantially mixed by spin–orbit coupling, the mixing has become large by 5.3 Å (10 bohr). The effect is particularly strong for the experimentally relevant $^2\Pi_{1/2}$ states, which undergo a complete alteration of character from predominately Π at R_e, to predominately Σ^* at infinite separation. The extent of this mixing will be strongly influenced by solvent effects and may be expected to play an important role in the dynamics of photodissociation. These effects will be the focus of upcoming investigations.

One final point of contention arises from the assignment of the Hund's case (a) labels in dissociative electron attachment experiments [9,10]. In these experiments, the fragment angular distributions show no evidence of mixing of different Λ states by spin–orbit coupling. This result is consistent with our observation that the Hund's case (a) character becomes dominant as the bond is shortened. In both studies, however, the highest energy peak has been assigned to a state of Π symmetry, in direct contradiction with the current calculations and other assignments based on the absorption spectra [5,11,13]. A crossing of the Σ^* and Π^* states cross at bondlengths shorter than R_e could account for this observation, but there is no evidence of such a crossing in the current calculations. Nevertheless, the absorption data and the current calculations strongly support the assignment of the highest electronic state as predominantly Σ in character at R_e.

4. Concluding remarks

We have carried out high-level calculations of the electronic states of I_2^- and ICl^- using an effective Hamiltonian to treat the strong effects of spin–orbit coupling. The results for both the transition frequencies and the extent of mixing due to spin–orbit effects appear to be in good agreement with experiments near the equilibrium geometry of the ground electronic state. The well depth for the ground electronic state is in error for both anions by about 20–30%, probably due to inadequacies in the basis sets used. Analysis of the wavefunctions reveals that the Hund's case (a) character of the wavefunctions is strong ($> 90\%$) at R_e but rapidly decreases as the bondlength increases. The details of this mixing as the bond dissociates are likely to be important in understanding photodissociation dynamics in clusters and the condensed phase.

Acknowledgements

We would like to thank John Papanikolas and Maria Nadal for helpful discussions. We also acknowledge Maria Nadal and Carl Lineberger for sharing their unpublished photodissociation data. This work was supported by Grants Nos. CHE-9217693, and PHY-9012244 from the National Science Foundation.

References

[1] J.M. Papanikolas, J.R. Gord, N.E. Levinger, D. Ray, V. Vorsa and W.C. Lineberger, J. Phys. Chem. 95 (1991) 8028.
[2] U. Banin, A. Waldman and S. Ruhman, J. Chem. Phys. 96 (1992) 2416.
[3] P.K. Walhout, J.C. Alfano, K.A.M. Thakur and P.F. Barbara, J. Phys. Chem. 99 (1995) 7568.
[4] M. Nadal, Ph.D. thesis, University of Colorado (1996).
[5] E.C.M. Chen and W.E. Wentworth, J. Phys. Chem. 89 (1985) 4099.
[6] D.J. Auerbach, M.M. Hubers, A.P.M. Baede and J. Los, Chem. Phys. 176 (1973) 107.
[7] U. Ross, T. Schulze and H.-J. Meyer, Chem. Phys. Lett. 121 (1985) 174.
[8] L. Bañares and A.G. Ureña, Chem. Phys. Lett. 176 (1991) 178.
[9] R. Azria, R. Abouaf and D. Teillet-Billy, J. Phys. B 21 (1988) L213.
[10] Y.L. Coat, J.-P. Guillotin and L. Bouby, J. Phys. B 24 (1991) 3285.

[11] C.J. Delbecq, W. Hayes and P.H. Yuster, Phys. Rev. 121 (1961) 1043.
[12] T. Shida, Y. Takahashi and H. Hatano, Chem. Phys. Lett. 33 (1975) 491.
[13] J.G. Dojahn, E.C.M. Chen and W.E. Wentworth, J. Phys. Chem. 100 (1996) 9649.
[14] P.W. Tasker, G.G. Balint-Kurti and R.N. Dixon, Mol. Phys. 32 (1976) 1651.
[15] G.A. Bowmaker, P. Schwerdtfeger and L. von Szentpaly, J. Mol. Struct. THEOCHEM 53 (1989) 87.
[16] D. Danonvich, J. Hrušák and S. Shaik, Chem. Phys. Lett. 233 (1995) 249.
[17] MOLPRO, a package of ab initio programs by H.-J. Werner and P.J. Knowles, with contributions from J. Almlöf, R.D. Amos, M.J.O. Deegan, S.T. Elbert, C. Hampel, W. Meyer, K. Peterson, R. Pitzer, A.J. Stone and P.R. Taylor, version 94.3 (1994).
[18] H.-J. Werner and P.J. Knowles, J. Chem. Phys. 89 (1988) 5803.
[19] P.J. Knowles and H.-J. Werner, Chem. Phys. Lett. 145 (1988) 514.
[20] H.-J. Werner and P.J. Knowles, J. Chem. Phys. 82 (1985) 5053.
[21] P.J. Knowles and H.-J. Werner, Chem. Phys. Lett. 115 (1985) 259.
[22] A. Sadlej, Theor. Chim. Acta 79 (1991) 123.
[23] A. Sadlej, Theor. Chim. Acta 81 (1992) 339.
[24] A.J. Stone, Chem. Phys. Lett. 83 (1981) 233.
[25] H. Lefebvre-Brion and R.W. Field, Perturbations in the spectra of diatomic molecules (Academic Press, Boston, 1986).
[26] G. Herzberg, Molecular spectra and molecular structure, Vol. I. Spectra of diatomic molecules, 2nd Ed. (Van Nostrand, New York, 1950) pp. 391–394.
[27] E.J. Heller, J. Chem. Phys. 68 (1978) 2066.
[28] T.M. Miller, Electron affinities, in: CRC handbook of chemistry and physics, 73rd Ed., ed. D.R. Lide (CRC Press, Boca Raton, 1993) pp. 10–180.
[29] C. Teichteil and M. Pelissier, Chem. Phys. 180 (1994) 1.
[30] G.N.R. Tripathi, R.H. Schuler and R.W. Fessenden, Chem. Phys. Lett. 113 (1985) 563.
[31] K.P. Huber and G. Herzberg, Molecular spectra and molecular structure, Vol. IV. Constants of diatomic molecules (Van Nostrand, New York, 1979).